Metal-Promoted Fusion of $B_6H_9^-$. Directed Synthesis and Structural Characterization of Dodecaborane(16), $B_{12}H_{16}$[1]

Cynthia T. Brewer, Robert G. Swisher, Ekk Sinn, and Russell N. Grimes*

Contribution from the Department of Chemistry, University of Virginia, Charlottesville, Virginia 22901. *Received December 5, 1984*

Abstract: The reaction of $K^+B_6H_9^-$ with $FeCl_2/FeCl_3$ in dimethyl ether at −78 °C produces $B_{12}H_{16}$, the first neutral B_{12} hydride, in 43% isolated yield. Dodecaborane(16), a colorless sublimable air-stable solid, was characterized from its IR and mass spectra, ^{11}B and ^1H FT NMR spectra, two-dimensional ^{11}B–^{11}B NMR spectrum, and an X-ray crystal structure determination. The cage skeleton is of the conjuncto type, consisting of open B_6 and B_8 units joined along a common B–B edge with their respective open faces on opposite sides of the molecule, and contains discrete B_6 pyramidal units, consistent with its formation via metal-mediated fusion of B_6 anions. There are ten terminal and six bridging hydrogens, two of the borons having only bridging H atoms attached. Treatment of $B_{12}H_{16}$ with KH in THF solution generates the $B_{12}H_{15}^-$ ion, which can be reprotonated with HCl to restore the original borane. The molecular structure and framework bonding are discussed in terms of both skeletal electron-counting and localized valence-bond descriptions. Crystal data are as follows: space group $Pna2_1$, a = 10.686 (3) Å, b = 8.686 (4) Å, c = 11.351 (4) Å, V = 1054 Å^3, R = 0.045 for 1021 reflections having $F_o > 3\sigma(F_o^2)$.

In the preceding paper,[2] we describe the facile transition-metal-assisted fusion of $B_5H_8^-$ ions and 5-vertex *nido*-cobaltaborane clusters to give 10-vertex nido products and of $B_{10}H_{13}^-$ ions to give $B_{18}H_{22}$. The basic strategy of cage construction via the stereochemically controlled assembly of smaller cage units thus seems quite general, at least for boron clusters, having now been successfully applied to carboranes, metallacarboranes, boranes, and metallaboranes.[2,3] In principle, this approach offers the boron chemist a way of synthesizing with reasonable efficiency new cage structures of specified geometry from available "building block" subunits, much as the organic chemist has done for years. The method should be especially useful in the synthesis of binary boron hydrides (having all-boron skeletons) since most of the known boranes were originally obtained serendipitously in complex, low-yield reactions. However, recently developed techniques involving stepwise addition of boron[4] have greatly improved the availability of several of the lower boranes, and acid–base reactions[5] or controlled hydrolysis[6] has generated several new hydrides in the B_{11}–B_{20} range.

In order to further test the viability of our method, we chose to attempt the preparation of a 12-vertex neutral borane, of which no examples existed,[7] via fusion of B_6 units. In this article, we report on the reaction itself as well as the structural elucidation and some chemistry of the dodecaborane product.[9]

Results and Discussion

The $B_6H_9^-$ anion, obtained[10] by deprotonation of B_6H_{10} with H^- in THF, was an obvious choice as the borane substrate, while $FeCl_2/FeCl_3$ was selected on economic grounds as the metal reagent[2] for our first attempts. A priori, the fused product was anticipated to be $B_{12}H_{16}$, a 28-skeletal electron system that is formally of the nido class and isoelectronic with the known $R_4C_4B_8H_8$ carboranes which form on fusion of $R_2C_2B_4H_4^{2-}$ ligands.[3] Additionally, the possible formation of $B_{12}H_{18}$ via a single B–B linkage of two B_6H_9 units was considered (analogous to the observed[2] formation of 2,2′-$(B_5H_8)_2$ as a side product in the fusion of $B_5H_8^-$); however, we hoped to minimize this process in favor of the fusion mechanism. Accordingly, a solution of $K^+B_6H_9^-$ in cold dimethyl ether was reacted with $FeCl_2$ to effect formation of a presumed ferraborane intermediate, after which $FeCl_3$ was added as an oxidizer. On workup, the reaction mixture gave only B_6H_{10}, and the desired new borane, $B_{12}H_{16}$, was isolated via extraction with *n*-hexane and sublimation in vacuo as colorless, air-stable crystals, mp 64–66 °C. The observation that B_6H_{10}, but little or no H_2, is produced supports the stoichiometry in eq 1, implying a 4:1 ratio of borane substrate to fused product as

$$\underset{9.2\ \text{mmol}}{4B_6H_9^-} + \underset{10.0}{4Fe^{3+}} \rightarrow \underset{1.0}{B_{12}H_{16}} + \underset{4.6}{2B_6H_{10}} + 4Fe^{2+} \quad (1)$$

was found in other borane fusions.[2] On this basis, the isolated yield of $B_{12}H_{16}$ is 43% after some loss of material during workup. The recovered B_6H_{10} can, of course, be recycled.

Table I. FT NMR Data on $B_{12}H_{16}$

assign	δ, ppm[a]	J_{BH}, Hz	rel area
	^{11}B (115.8 MHz)[b]		
B(7)–H	15.35	193	1
B(4,6)–H	13.41	203	2
B(5)–H	11.39	213	1
B(9,10)–H, B(2,3)–H	4.53	*c*	4
B(8,11)–H	−18.37	150	2
B(1)–H	−40.78	156	1
B(12)–H	−43.10	159	1
	^1H (360 MHz)[d]		
B–H_{term}	4.76	151	2
B–H_{term}	3.95	156	2
B–H_{term}	~3.40	~150	2
B–H_{term}	2.41	148	2
B–H_{term}	0.93	157	1
B–H_{term}	−2.40	154	1
B–H–B	~−1.5	*c*	5
B–H–B	~−2.0	*c*	
B–H–B	~−2.8	*c*	1

[a] Chemical shift relative to $BF_3{\cdot}O(C_2H_5)_2$ for ^{11}B spectrum, to $Si(CH_3)_4$ for ^1H spectrum. [b] *n*-Hexane solution. [c] J not measurable. [d] C_6D_6 solution.

Spectroscopic Characterization of $B_{12}H_{16}$. The electron-impact (EI) mass spectrum exhibits a high mass cutoff at m/e 148 corresponding to the $^{11}B_{12}H_{16}^+$ ion, but with extensive loss of hydrogen (base peak at m/e 138). The chemical ionization (CI)

(1) Based in part on: Brewer, C. T. Ph.D. Dissertation, University of Virginia, 1984.
(2) Brewer, C. T.; Grimes, R. N. *J. Am. Chem. Soc.*, preceding paper in this issue.
(3) (a) Grimes, R. N. *Acc. Chem. Res.* **1983**, *16*, 22. (b) *Adv. Inorg. Chem. Radiochem.* **1983**, *26*, 55 and references therein.
(4) Toft, M. A.; Leach, J. B.; Himpsl, F. L.; Shore, S. G. *Inorg. Chem.* **1982**, *21*, 1952.
(5) (a) Huffman, J. C.; Moody, D. C.; Schaeffer, R. *Inorg. Chem.* **1981**, *20*, 741. (b) *Ibid.* **1976**, *15*, 227. (c) Rathke, J.; Schaeffer, R. *Ibid.* **1974**, *13*, 3008. (d) Rathke, J.; Schaeffer, R. *J. Am. Chem. Soc.* **1973**, *95*, 3402.
(6) Hermanek, S.; Fetter, K.; Plesek, J.; Todd, L. J.; Garber, A. R. *Inorg. Chem.* **1975**, *14*, 2250.
(7) Although B_{12} icosahedra are pervasive structural units in elemental boron,[8] the only previously characterized 12-boron molecular species are the $B_{12}H_{12}^{2-}$ ion and its derivatives.
(8) Greenwood, N. N. "The Chemistry of Boron"; Pergamon Press: Oxford, 1973 and references therein.
(9) A preliminary report of this work has appeared: Brewer, C. T.; Grimes, R. N. *J. Am. Chem. Soc.* **1974**, *106*, 2722.
(10) Johnson, H. D.; Shore, S. G.; Mock, N. L.; Carter, J. C. *J. Am. Chem. Soc.* **1969**, *91*, 2131.

0002-7863/85/1507-3558$01.50/0

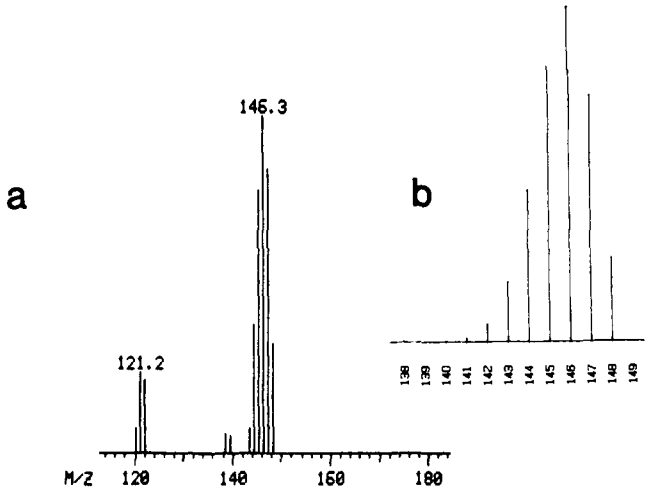

Figure 1. (a) Chemical ionization mass spectrum of $B_{12}H_{16}$ in CH_4. (b) Calculated spectrum based on natural isotopic abundances.

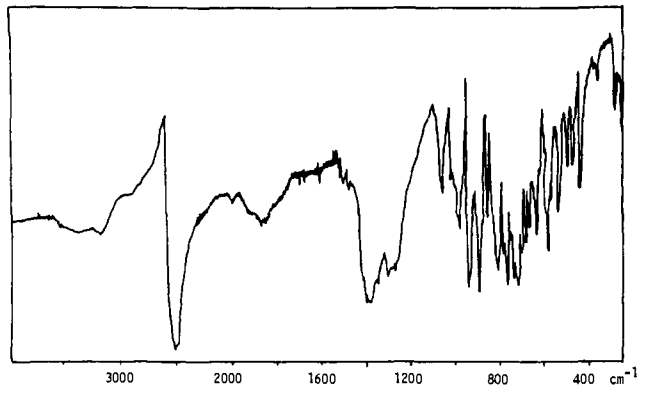

Figure 2. Infrared spectrum of $B_{12}H_{16}$ (KBr pellet).

spectrum in methane, however, contains an intense parent grouping whose intensities correspond closely to the pattern calculated from natural isotopic abundances (Figure 1).

The infrared spectrum in KBr (Figure 2) contains absorptions typical of B–H terminal and B–H–B bridging stretching vibrations near 2500 and 1900 cm^{-1}, respectively, but otherwise conveys little structural information. The 115.8-MHz ^{11}B FT NMR spectrum (Table I and Figure 3) reveals a singlet of area 4 and six doublets, each of which collapses to a singlet on proton-decoupling. The area-4 peak is slightly broadened in the coupled spectrum, suggesting that it arises from superposition of two nonequivalent resonances, one of which may be a singlet; this would imply the presence of borons having no attached terminal hydrogens. Overall, the spectrum is consistent with a framework of mirror symmetry containing four unique BH units. The 360-MHz proton spectrum (Table I and Figure 4) contains a pattern of overlapping quartets arising from coupling of B–H terminal protons to spin $-{}^3/_2$ ^{11}B nuclei. The high-field region of the spectrum (δ −1.0 to −3.5) exhibits three broad signals attributed to B–H–B bridging groups, superimposed on a B–H terminal quartet.

These spectral data support an open-cage structure of C_s symmetry, consistent with the prediction of nido geometry for a 28-skeletal electron $2n + 4$ cluster,[11] but they do not reveal the actual molecular architecture. Additional insight, however, was given by the two-dimensional (2D) homonuclear ^{11}B–^{11}B NMR spectrum[12] shown in Figure 5. The peaks along the diagonal represent the normal (1D) ^{11}B spectrum and occur at the same chemical shifts (compare with Figure 3). The off-diagonal or cross peaks reveal direct scalar coupling between boron nuclei[12] and are observable only where electron density, hence bonding, exists. Given such information, it is often possible to deduce the framework connectivity in a molecule. In this case, there are some complications, however: peak D (δ 4.5 ppm) is evidently a superposition of two resonances (vide supra), and peak C exhibits no clear cross peaks with other resonances. Despite these difficulties, the data can be interpreted. From the 1D spectrum (Figure 3), it is clear that A, C, F, and G are unique and hence located on the mirror; further, A and G are directly linked, as their mutual cross peak attests. The pattern of connectivities deduced from cross peaks indicates that A, D, E, and G are completely interconnected. This would be structurally unreasonable, but as "D" contains superimposed resonances as discussed above, it is clear that the cross peaks involving "D" actually arise from two different pairs of boron nuclei which we label D and D′. A connectivity diagram summarizing this information without regard to symmetry is given in Figure 6a, and introduction of the mirror plane leads to the complete boron skeleton, Figure 6b. In this diagram, connections between equivalent borons (e.g., D′–D′) must be assumed since the 2D experiment cannot reveal their mutual coupling;[12] also, there is ambiguity involving atoms D and D′, whose resonances are superimposed. Two additional problems remain: the locations of the bridging hydrogens and the absence of the expected cross peak between atoms C and F. Since studies on other boranes have shown that cross peaks between boron atoms linked via B–H–B bridges are usually absent,[12,13] likely locations for these protons are along the pairs of B–C, B–D′, and D–D edges, which lie on the open faces of the molecule.

The missing cross peak is not reasonably explained on the basis of a B–H–B bridge between atoms C and F, as the C–F edge is

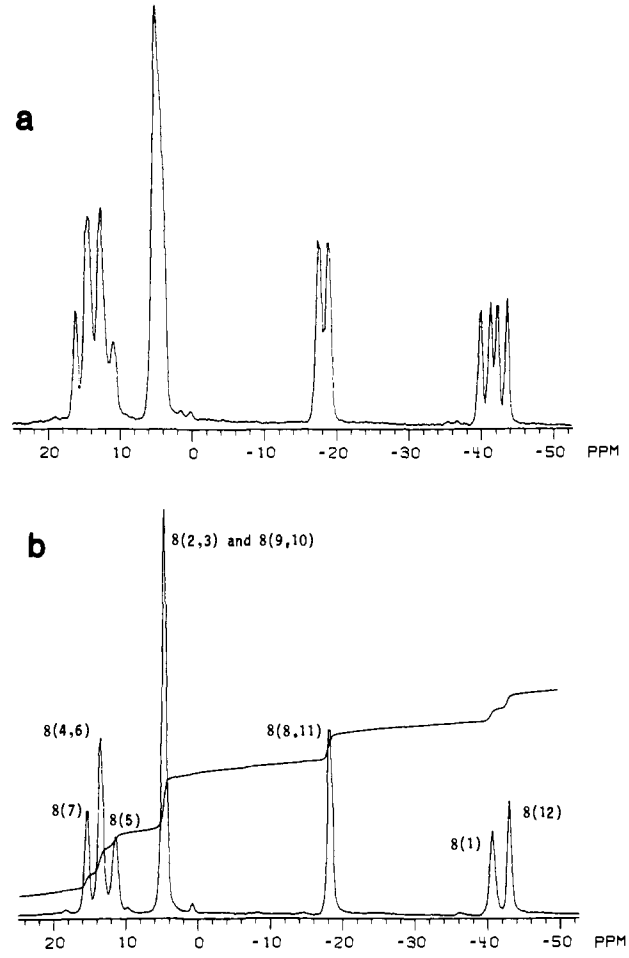

Figure 3. ^{11}B FT NMR spectra (115.8 MHz) of $B_{12}H_{16}$ in *n*-hexane. (a) Proton-coupled. (b) Proton-decoupled. For a discussion of the assignments, see text.

(11) O'Neill, M. E.; Wade, K. In "Metal Interactions with Boron Clusters"; Grimes, R. N., Ed.; Plenum Press: New York, 1983; Chapter 1 and references therein. (b) Mingos, D. M. P. *Acc. Chem. Res.* **1984**, *17*, 311.

(12) Venable, T. .; Hutton, W. C.; Grimes, R. N. *J. Am. Chem. Soc.* **1984**, *106*, 29.

(13) Reed, D. *J. Chem. Res.* **1984**, 198.

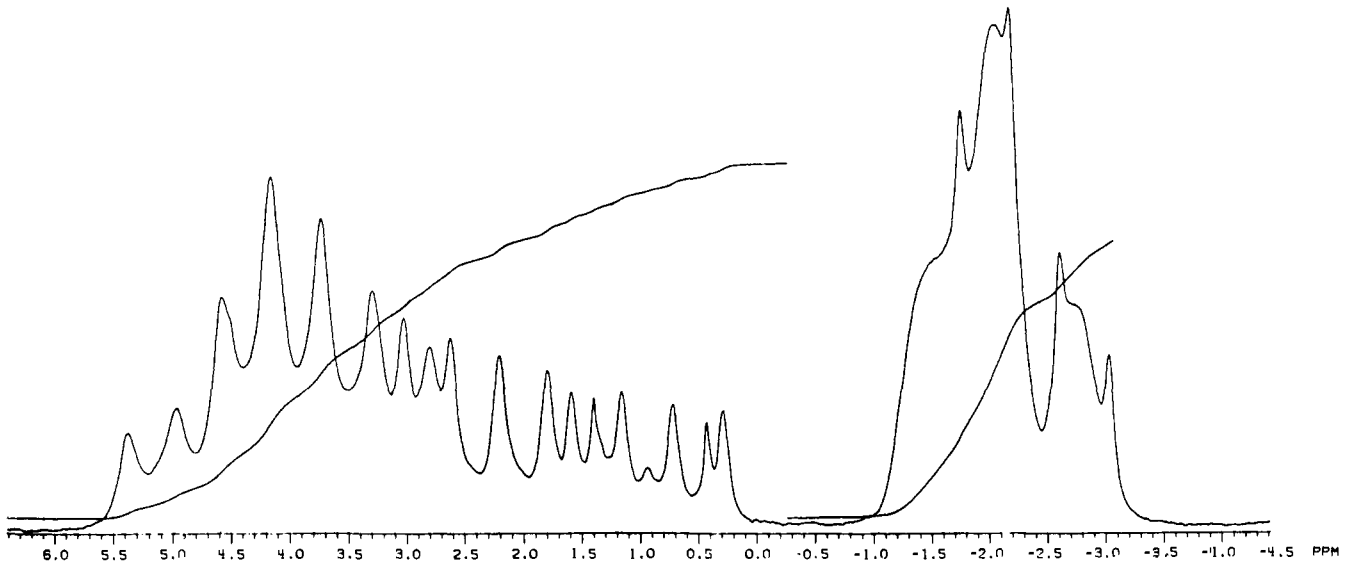

Figure 4. ^{1}H FT NMR spectrum (360 MHz) of $B_{12}H_{16}$ in C_6D_6 solution.

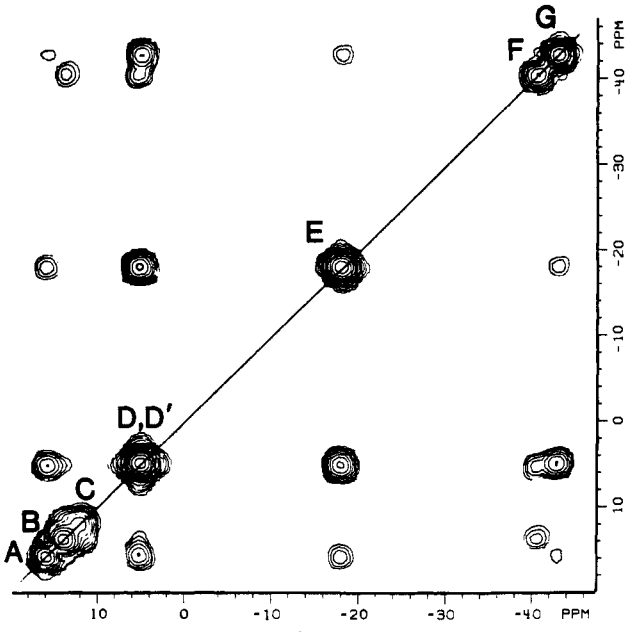

Figure 5. Two-dimensional (2D) ^{11}B–^{11}B NMR spectrum (115.8 MHz) in *n*-hexane.

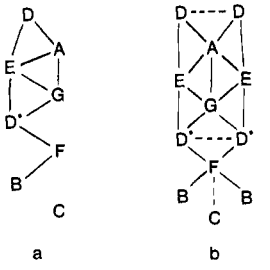

Figure 6. Connectivity diagrams of $B_{12}H_{16}$ derived from 2D NMR data. (a) Asymmetric unit of molecule. (b) Full molecule (dashed lines indicate presumed bonds that are not directly observable).

not on an open rim; to our knowledge, there is no precedent for hydrogen bridging on a nonrim B–B edge in an open-cage framework. Another possible explanation, that of a very short longitudinal relaxation time (T_1) for resonance C, was examined via T_1 measurements of all peaks in the ^{11}B spectrum except the overlapped D and D′ signals. The measured T_1 values of resonances A–G, excluding D, are, respectively, 30, 14, 11, 25, 89, and 47 ms; thus, the shortest value measured is indeed that of C, but it is still within an order of magnitude of the other T_1's

Table II. Experimental Parameters and Crystal Data

space group	$Pna2_1$	D(calcd), g cm^{-3}	0.919
a, Å	10.686 (3)	μ, cm^{-1}	0.36
b, Å	8.686 (4)	esd unit wt	0.39
c, Å	11.351 (4)	R	0.045
V	1054	R_w	0.044
Z	4	radiation	Mo Kα

in the molecule. However, an alternative possibility is that the transverse relaxation time T_2 is unusually short for C, leading to rapid decay of the cross peak intensity for couplings involving C. The fact that this peak is the broadest in the spectrum (indicative of a short T_2) lends some support to this idea. Other examples of "missing cross peak" phenomena have been noted and discussed in detail earlier.[12]

The connectivity pattern given in Figure 6b has the geometry of 6-vertex and 8-vertex nido cages sharing a common edge and is quite compatible with the actual synthesis of the molecule via fusion of two pentagonal pyramidal B_6 units (see discussion below). The application of 2D ^{11}B–^{11}B NMR to the elucidation of the cage geometry of $B_{12}H_{16}$ provides a convincing demonstration, in our view, of the extraordinary potential of the method for structural characterization of new species. It also illustrates some limitations, since the 2D data do not reveal the full three-dimensional geometry or the location of bridging hydrogen atoms. In order to complete the picture, an X-ray crystallographic study was undertaken.

X-ray Structure Determination of $B_{12}H_{16}$. Crystal data and parameters of the data collection are given in Table II, while Tables III–V list atom coordinates, bond distances and angles, and calculated mean planes. The molecular structure (Figure 7) is consistent with the boron framework deduced from the 2D NMR evidence described above, consisting of two B_6 nido cages joined at their bases; however, the two B_6 units are mutually inverted such that their open sides face away from one another. The basal planes of the B_6 pyramids are inclined at an angle of 110.7°; as a consequence, H(1) [attached to the apex boron B(1)] is almost centered over the basal plane of the other B_6 unit, defined by B(7)–B(8)–(B9)–B(10)–B(11).

There are six bridging hydrogens, and hence two of the borons, B(2) and B(3), have no terminal hydrogen atoms. However, atoms H(26) and H(34) could be considered quasi-terminal since they are closer to B(2) and B(3), respectively, than to B(4) and B(6). The structure as deduced from X-ray evidence is asymmetric because of the unique bridging hydrogen H(45), but if H(45) tautomerizes in solution between the equivalent B(4)–B(5) and B(5)–B(6) edges, this would produce time-averaged C_s symmetry with vertices 1, 5, 7, and 12 on the mirror plane, in agreement with the NMR data previously discussed. There are no unusual B–B or B–H bond distances in the molecule, and it is reassuring

Table III. Positional Parameters

atom	*x*	*y*	*z*
B(1)	0.1021 (3)	0.3797 (4)	0.6688 (3)
B(2)	0.0122 (3)	0.2179 (4)	0.6313 (3)
B(3)	0.1221 (3)	0.2020 (4)	0.7399 (3)
B(4)	0.2547 (3)	0.3039 (4)	0.6939 (4)
B(5)	0.2173 (3)	0.3807 (5)	0.5569 (4)
B(6)	0.0709 (4)	0.3301 (5)	0.5174 (3)
B(7)	0.0069 (3)	0.0679 (3)	0.7282 (3)
B(8)	0.0506 (3)	0.1395 (4)	0.8732 (3)
B(9)	−0.0795 (3)	0.2472 (4)	0.9284 (4)
B(10)	−0.1917 (3)	0.2630 (5)	0.8189 (4)
B(11)	−0.1369 (3)	0.1638 (4)	0.6894 (3)
B(12)	−0.1117 (3)	0.0923 (4)	0.8388 (3)
H(1)	0.064 (2)	0.490 (3)	0.713 (2)
H(4)	0.338 (2)	0.336 (3)	0.756 (2)
H(5)	0.266 (3)	0.473 (3)	0.519 (3)
H(6)	0.014 (3)	0.380 (3)	0.441 (3)
H(7)	0.024 (2)	−0.054 (3)	0.702 (2)
H(8)	0.098 (2)	0.075 (3)	0.940 (3)
H(9)	−0.103 (3)	0.264 (3)	1.019 (3)
H(10)	−0.283 (3)	0.286 (3)	0.835 (3)
H(11)	−0.212 (2)	0.112 (3)	0.632 (2)
H(12)	−0.160 (2)	−0.002 (3)	0.870 (2)
H(26)	0.049 (3)	0.180 (3)	0.535 (3)
H(34)	0.225 (3)	0.163 (3)	0.713 (3)
H(45)	0.274 (3)	0.295 (4)	0.592 (3)
H(89)	0.031 (3)	0.272 (3)	0.907 (3)
H(910)	−0.123 (3)	0.359 (3)	0.872 (3)
H(1011)	−0.163 (3)	0.295 (3)	0.720 (3)

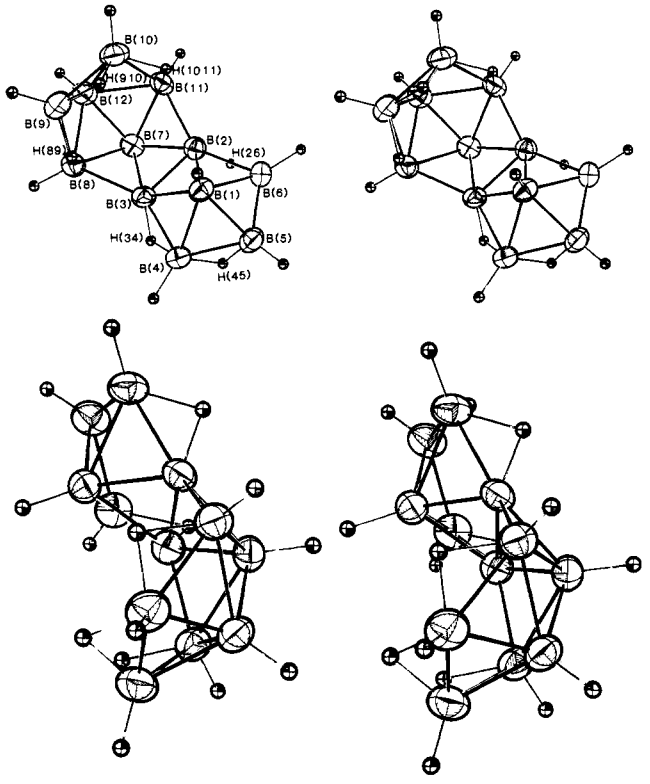

Figure 7. Stereoviews of $B_{12}H_{16}$ molecule showing all atoms.

to note that the B(1)–B(5) length [1.769 (8) Å] is clearly bonding despite the absence of a cross peak between these nuclei in the 2D boron NMR spectrum (vide supra).

The geometry of $B_{12}H_{16}$ is reminiscent of previously characterized conjuncto-boranes, which consist of cage units joined along a common edge. Among these are $B_{14}H_{20}$,[5a] $B_{13}H_{19}$,[5b] $B_{14}H_{18}$,[6] $B_{16}H_{20}$,[14] and *n*- and *i*-$B_{18}H_{22}$,[15] of which all but the first are similar to $B_{12}H_{16}$ in that their open faces are oriented in roughly opposite directions. In addition, there are several metallaboranes of the conjuncto class.[16]

Table IV. Interatomic Distances and Angles

		Distances, Å			
B(1)	B(2)	1.755 (8)	B(11)	B(12)	1.826 (9)
B(1)	B(3)	1.754 (8)	B(1)	H(1)	1.154 (45)
B(1)	B(4)	1.781 (9)	B(2)	H(26)	1.203 (57)
B(1)	B(5)	1.769 (8)	B(3)	H(34)	1.192 (51)
B(1)	B(6)	1.802 (10)	B(4)	H(4)	1.167 (49)
B(2)	B(3)	1.708 (8)	B(4)	H(34)	1.278 (48)
B(2)	B(6)	1.736 (9)	B(4)	H(45)	1.176 (50)
B(2)	B(7)	1.706 (8)	B(5)	H(5)	1.047 (53)
B(2)	B(11)	1.788 (8)	B(5)	H(45)	1.039 (50)
B(3)	B(4)	1.750 (8)	B(6)	H(6)	1.144 (59)
B(3)	B(7)	1.700 (8)	B(6)	H(26)	1.345 (56)
B(3)	B(8)	1.780 (8)	B(7)	H(7)	1.114 (42)
B(4)	B(5)	1.738 (10)	B(8)	H(8)	1.068 (50)
B(5)	B(6)	1.686 (9)	B(8)	H(89)	1.233 (54)
B(7)	B(8)	1.820 (9)	B(9)	H(9)	1.070 (63)
B(7)	B(11)	1.803 (8)	B(9)	H(89)	1.221 (52)
B(7)	B(12)	1.796 (9)	B(9)	H(910)	1.253 (54)
B(8)	B(9)	1.789 (9)	B(10)	H(10)	1.015 (58)
B(8)	B(12)	1.824 (8)	B(10)	H(910)	1.257 (54)
B(9)	B(10)	1.732 (11)	B(10)	H(1011)	1.198 (64)
B(9)	B(12)	1.721 (10)	B(11)	H(11)	1.128 (52)
B(10)	B(11)	1.801 (10)	B(11)	H(1011)	1.224 (60)
B(10)	B(12)	1.726 (9)	B(12)	H(12)	1.032 (51)

			Angles (deg)				
B(2)	B(1)	B(3)	58.2 (3)	B(2)	B(7)	B(12)	112.6 (4)
B(2)	B(1)	B(4)	104.1 (4)	B(3)	B(7)	B(9)	60.7 (3)
B(2)	B(1)	B(5)	102.2 (5)	B(3)	B(7)	B(11)	108.6 (4)
B(2)	B(1)	B(6)	58.4 (4)	B(3)	B(7)	B(12)	112.1 (4)
B(3)	B(1)	B(4)	59.3 (3)	B(8)	B(7)	B(11)	106.4 (4)
B(3)	B(1)	B(5)	104.5 (4)	B(8)	B(7)	B(12)	60.6 (3)
B(3)	B(1)	B(6)	104.5 (4)	B(11)	B(7)	B(12)	61.0 (4)
B(4)	B(1)	B(5)	58.6 (4)	B(3)	B(8)	B(7)	56.3 (4)
B(4)	B(1)	B(6)	103.5 (5)	B(3)	B(8)	B(9)	118.2 (4)
B(5)	B(1)	B(6)	56.3 (4)	B(3)	B(8)	B(12)	107.1 (4)
B(1)	B(2)	B(3)	60.9 (3)	B(7)	B(8)	B(9)	107.2 (4)
B(1)	B(2)	B(6)	62.2 (4)	B(7)	B(8)	B(12)	59.1 (3)
B(1)	B(2)	B(7)	118.2 (4)	B(9)	B(8)	B(12)	56.9 (4)
B(1)	B(2)	B(11)	127.5 (4)	B(8)	B(9)	B(10)	109.1 (5)
B(3)	B(2)	B(6)	109.6 (4)	B(8)	B(9)	B(12)	62.6 (4)
B(3)	B(2)	B(7)	59.7 (3)	B(10)	B(9)	B(12)	60.0 (4)
B(3)	B(2)	B(11)	109.0 (4)	B(9)	B(10)	B(11)	108.8 (5)
B(6)	B(2)	B(7)	157.1 (5)	B(9)	B(10)	B(12)	59.7 (4)
B(6)	B(2)	B(11)	138.1 (5)	B(11)	B(10)	B(12)	62.3 (4)
B(7)	B(2)	B(11)	62.1 (3)	B(2)	B(11)	B(7)	56.7 (3)
B(1)	B(3)	B(2)	60.9 (3)	B(2)	B(11)	B(10)	117.7 (5)
B(1)	B(3)	B(4)	61.1 (3)	B(2)	B(11)	B(12)	107.5 (4)
B(1)	B(3)	B(7)	118.6 (4)	B(7)	B(11)	B(10)	107.3 (5)
B(1)	B(3)	B(8)	127.4 (4)	B(7)	B(11)	B(12)	59.3 (4)
B(2)	B(3)	B(4)	107.5 (4)	B(10)	B(11)	B(12)	56.8 (4)
B(2)	B(3)	B(7)	60.1 (3)	B(7)	B(12)	B(8)	60.4 (3)
B(2)	B(3)	B(8)	110.1 (4)	B(7)	B(12)	B(9)	111.3 (4)
B(4)	B(3)	B(7)	155.4 (5)	B(7)	B(12)	B(10)	111.0 (5)
B(4)	B(3)	B(8)	139.1 (5)	B(7)	B(12)	B(11)	59.7 (3)
B(7)	B(3)	B(8)	63.0 (4)	B(8)	B(12)	B(9)	60.5 (4)
B(1)	B(4)	B(3)	59.6 (3)	B(8)	B(12)	B(10)	107.8 (5)
B(1)	B(4)	B(5)	60.3 (4)	B(8)	B(12)	B(11)	105.2 (4)
B(3)	B(4)	B(5)	106.0 (5)	B(9)	B(12)	B(10)	60.3 (4)
B(1)	B(5)	B(4)	61.0 (1)	B(9)	B(12)	B(11)	108.2 (4)
B(1)	B(5)	B(6)	62.8 (4)	B(10)	B(12)	B(11)	60.9 (4)
B(4)	B(5)	B(6)	110.6 (5)	B(2)	H(26)	B(6)	85.7 (4)
B(1)	B(6)	B(2)	59.4 (3)	B(3)	H(34)	B(4)	90.2 (3)
B(1)	B(6)	B(5)	60.8 (4)	B(4)	H(45)	B(5)	103.2 (5)
B(2)	B(6)	B(5)	106.5 (5)	B(8)	H(89)	B(9)	93.6 (4)
B(2)	B(7)	B(3)	60.2 (4)	B(9)	H(910)	B(10)	87.3 (3)
B(2)	B(7)	B(8)	108.3 (4)	B(10)	H(1011)	B(11)	96.1 (5)
B(2)	B(7)	B(11)	61.2 (3)				

(14) (a) Friedman, L. B.; Cook, R. E.; Glick, M. D. *Inorg. Chem.* **1970**, *9*, 1452. (b) Plesek, J.; Hermanek, S.; Hanousek, F. *Collect. Czech. Chem. Commun.* **1967**, *33*, 699.

(15) (a) Pitochelli, A. R.; Hawthorne, M. F.; *J. Am. Chem. Soc.* **1962**, *84*, 3218. (b) Simpson, P. G.; Lipscomb, W. N. *J. Chem. Phys.* **1963**, *39*, 26. (c) Simpson, P. G.; Folting, K.; Dobrott, R. D. *Ibid.* **1963**, *39*, 2339.

(16) For a recent review of metallaboranes, see: Greenwood, N. N. *Pure Appl. Chem.* **1983**, *55*, 1415.

Table V. Selected Mean Planes and Dihedral Angles between Planes

atom	dev, Å	atom	dev, Å
Plane 1: B(2), B(3), B(7)			
$0.5870x - 0.5414y - 0.6106z = -5.3090$			
B(2)	0	B(7)	0
B(3)	0	B(1)	−0.466
Plane 2: B(1), B(2), B(3)			
$0.6844x - 0.2614y - 0.6807z = -5.2655$			
B(1)	0	B(3)	0
B(2)	0	B(7)	−0.448
Plane 3: B(2), B(3), B(8), B(12), B(11)			
$0.2051x - 0.9337y - 0.2936z = -3.8579$			
B(2)	0.021	B(1)	−1.219
B(3)	0.029	B(4)	−0.354
B(8)	−0.065	B(5)	−0.602
B(11)	0.076	B(6)	−0.381
B(12)	−0.061	B(7)	0.903
Plane 4: B(1), B(5), B(7), B(12)			
$-0.7037x + 0.8077y - 0.7050z = -5.7982$			
B(1)	−0.015	H(1)	0.003
B(5)	0.014	H(5)	0.021
B(7)	−0.012	H(7)	−0.023
B(12)	0.013	H(12)	0.057
Plane 5: B(7), B(8), B(9), B(10), B(11)			
$0.4556x + 0.8170y - 0.3534z = -2.3212$			
B(7)	−0.076	H(8)	−0.432
B(8)	0.064	H(9)	−0.382
B(9)	−0.027	H(10)	−0.362
B(10)	−0.021	H(11)	−0.449
B(11)	0.061	H(89)	0.771
B(12)	−0.923	H(910)	0.775
H(7)	−0.751	H(1011)	0.741
Plane 6: B(2), B(3), B(4), B(5), B(6)			
$0.3582x - 0.8227y - 0.4414z = -4.6667$			
B(2)	0.005	H(4)	−0.223
B(3)	−0.006	H(5)	−0.283
B(4)	0.004	H(6)	−0.196
B(5)	−0.001	H(26)	0.900
B(6)	−0.003	H(34)	0.800
B(1)	−0.995	H(45)	0.642

planes	angle, deg	planes	angle, deg
1,2	17.7	2,6	40.5
1,3	36.6	3,4	91.1
1,4	91.4	3,5	124.4
1,5	87.9	3,6	13.8
1,6	22.8	4,5	90.0
2,3	54.3	4,6	90.8
2,4	91.4	5,6	110.7
2,5	70.2		

^{11}B NMR Assignments. The combination of X-ray diffraction and 2D ^{11}B–^{11}B NMR data permits assignment of the individual resonances in the ^{11}B spectrum as given in Figure 3. The connectivities revealed in the 2D spectrum establish that peaks B, C, E, and F correspond, respectively, to B(4,6), B(5), B(8,11), and B(1). However, an ambiguity exists with respect to the other assignments because peaks D and D′ are superimposed; hence atom F in the connectivity diagram (Figure 6b) could be attached either to the D–D or the D′–D′ edge. As a consequence, the lowest- and highest-field peaks (A and G, respectively) could arise either from B(12) and B(7), respectively, or the reverse. It is known that apex borons in pyramidal borane frameworks tend to resonate at higher field;[17] for example, B(1) in B_6H_{10} appears at δ −52 while the basal borons resonate at δ +14.[18] Since B(12) is the apical atom of one of the hexaborane moieties in $B_{12}H_{16}$ [B(1) being the apex of the other], it is reasonable to assign the high-field resonance to B(12) and the low-field peak to B(7). As a caveat, however, we note that B(7) also has "apical" character in that its ring of attached atoms—B(2)–B(3)–B(8)–B(12)–B(11)—form the base of a pyramidal array; hence the assignments of B(12) and B(7) are not certain.

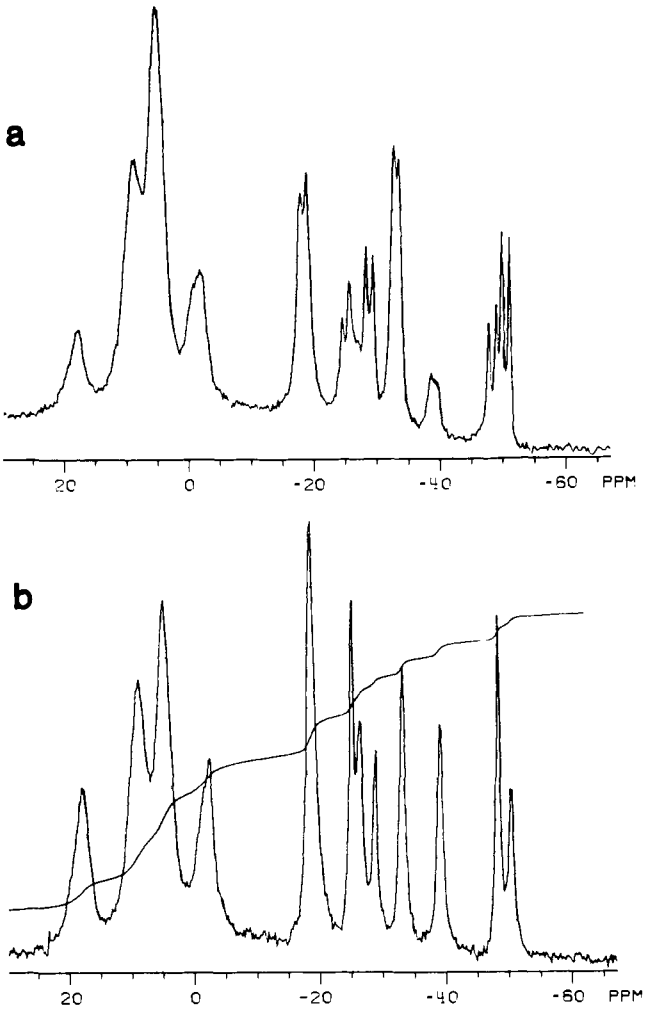

Figure 8. ^{11}B FT NMR spectra (115.8 MHz) of $K^+B_{12}H_{15}^-$ species at −78 °C in THF solution. (a) Proton-coupled. (b) Proton-decoupled.

Chemical Properties. Dodecaborane(16) is sublimable in vacuo and is moderately air-stable, but decomposes slowly at room temperature, forming a yellow solid; under refrigeration, it can be stored indefinitely without change. On treatment with KH in THF solution, $B_{12}H_{16}$ acts as a monoprotic acid, evolving an equivalent of hydrogen:

$$B_{12}H_{16} + KH \rightarrow K^+B_{12}H_{15}^- + H_2 \quad (2)$$

The ^{11}B NMR spectrum of the anion at −78 °C (Figure 8) indicates the presence of two species, one of which disappears (via decomposition or isomerization) to leave a single stable isomer at room temperature. The spectrum of the stable $B_{12}H_{15}^-$ ion, shown in Figure 9, exhibits a 2:4:1:1:1:2:1 pattern (expressed as relative areas) which strongly implies that the symmetry of the neutral borane is retained. Indeed, the reaction of $B_{12}H_{15}^-$ with anhydrous HCl regenerates the original $B_{12}H_{16}$ hydride. Comparison of the spectrum of the anion with that of $B_{12}H_{16}$ (Figure 3), however, indicates substantial shifts of several resonances, implying that bridge deprotonation significantly (but reversibly) alters the framework electron density distribution. The proton removed can safely be assumed to be of the bridging type, and the spectra support this; however, there is presently no way to identify its precise location.

The known structure of neutral $B_{12}H_{16}$ suggests that it may be susceptible to protonation to give $B_{12}H_{17}^+$, which would be a counterpart of the $B_6H_{11}^+$ ion, obtained via protonation of B_6H_{10}.[19]

(17) Eaton, G. R.; Lipscomb, W. N. "NMR Studies of Boron Hydrides and Related Compounds"; Benjamin: New York, 1969.
(18) Todd, L. J.; Siedle, A. R. *Prog. NMR Spectrosc.* **1979**, *13*, 87.
(19) Johnson, H. D., II; Brice, V. T.; Brubaker, G. L.; Shore, S. G. *J. Am. Chem. Soc.* **1972**, *94*, 6711.

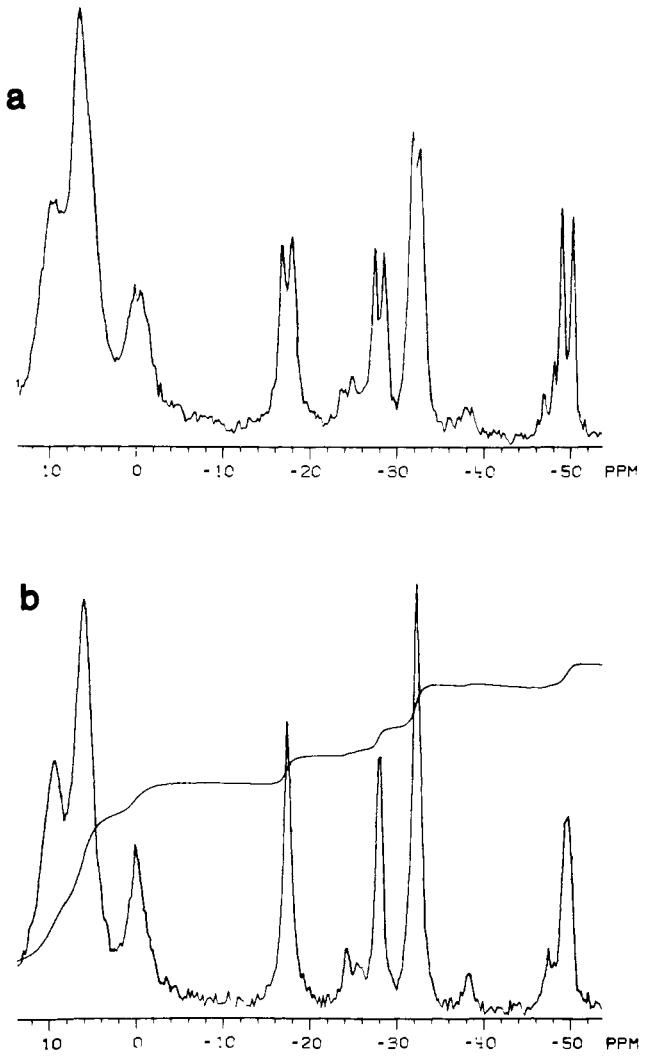

Figure 9. ^{11}B FT NMR spectra (115.8 MHz) of $K^+B_{12}H_{15}^-$ (stable isomer) at 25 °C in THF solution. (a) Proton-coupled. (b) Proton-decoupled.

However, $B_{12}H_{16}$ appears substantially unreactive toward HCl, and we have not, at this point, seen evidence for $B_{12}H_{17}^+$.

Formation of $B_{12}H_{16}$ and Discussion of Framework Bonding. In contrast to our earlier work on carborane fusion,[3,20] it has not been possible to isolate and characterize any of the metal–borane intermediate complexes involved in the fusion of the borane anions (although there is evidence of catalytic activity by metallaborane species obtained from transition-metal ions and $B_5H_8^-$ or $B_3H_8^-$ in the hydrogenation of alkenes and alkynes[21]). Nevertheless, both the structure of $B_{12}H_{16}$ and the analogy with the fusion of $R_2C_2B_4H_4^{2-}$ ligands to give $R_4C_4B_8H_8$[20] suggest thaat the formation of $B_{12}H_{16}$ from $B_6H_9^-$ involves a bis(borane) iron species of the type $Fe(B_6H_x)_2^{n-}$. In such complexes, the metal–ligand binding is likely to be via B–B edges rather than "sandwich"-type bonding involving the entire five-membered face of the B_6 pyramid (Figure 10); the presence of bridging hydrogen atoms makes the latter arrangement unlikely. From the known geometry of the fused borane, we infer that the ligands are probably oriented in transoid fashion (Figure 10a) as opposed to a cisoid geometry (Figure 10b). The latter arrangement would have considerably greater repulsive interaction between the hydrogen bridges on the two ligands and is presumably less favored for this reason. As we have speculated elsewhere,[22] fusion of the ligands probably begins via formation of a direct B–B link between them (for which

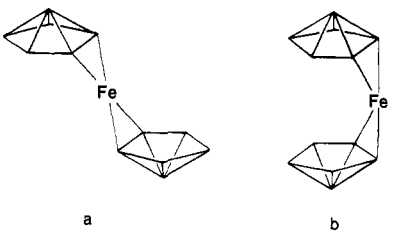

Figure 10. Possible geometries for $Fe(B_6H_x)_2$ intermediate in formation of $B_{12}H_{16}$.

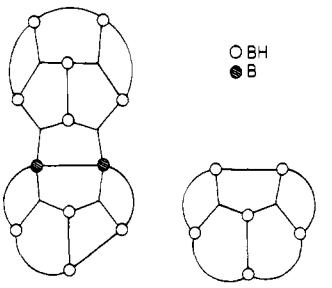

Figure 11. (Left) Topological structure of $B_{12}H_{16}$ showing three-center B–B–B, two-center B–B, and three-center B–H–B bonds. The latter are depicted as curved lines. (Right) Topological structure of B_6H_{10},[23] shown for comparison.

evidence has been found in other systems[22]), followed by solvent-assisted ejection of the metal ion. The fusion mechanism is clearly an important question which, however, presents some formidable experimental problems.[20]

Finally, we briefly consider the bonding within the $B_{12}H_{16}$ cage. As was noted earlier, from the viewpoint of skeletal electron counting, the molecule is a 28-electron nido system which is isoelectronic with the four-carbon carborane $C_4B_8H_{12}$ and its $R_4C_4B_8H_8$ (R = alkyl) derivatives. This implies that two electrons might be removed to give the hypothetical $B_{12}H_{16}^{2+}$ dication, a 26-electron cage which is expected to have regular icosahedral geometry (indeed, $B_{12}H_{16}^{2+}$ would be formally a tetraprotonated derivative of the known icosahedral species $B_{12}H_{12}^{2-}$). However, despite the similarity in skeletal electron population, $B_{12}H_{16}$ is structurally quite distinct from these icosahedral and near-icosahedral systems, and a localized-bond description seems appropriate. Figure 11 presents a valence-bond topological structure for $B_{12}H_{16}$ in terms of two- and three-center bonds, which corresponds to a 6620 styx formula[23,24] where the four digits give, respectively, the number of B–H–B bridges (s), three-center B–B–B bonds (t), two-center B–B bonds (y), and BH_2 groups (x). For comparison, the favored[23] styx representation for B_6H_{10} is depicted also. Viewed in this way, one can describe $B_{12}H_{16}$ as a B_6H_8 unit (a) to which a second B_6H_8 cage (b) has been attached via two three-center B–B–B bonds, with concomitant transfer of a bridging hydrogen from a to b. In this description, the two hexaborane groups are bound together by just two electron pairs, but thermal isomerization to a cisoid-type geometry with loss of two bridge hydrogens might induce closure of the cage into a more compact polyhedral structure. Fortunately, the relative accessibility of $B_{12}H_{16}$ permits examination of this and other possibilities.

Experimental Section

Materials and Instrumentation. Hexaborane(10) was prepared B_5H_9 and B_2H_6 by the method of Shore et al.[25] Potassium and sodium hydrides were obtained as dispersions in mineral oil and were washed with hexane prior to use. Tetrahydrofuran (THF) was dried over lithium aluminum hydride and distilled under vacuum, and preparative-layer

(20) Maynard, R. B.; Grimes, R. N. *J. Am. Chem. Soc.* **1982**, *104*, 5983 and references therein.
(21) Grimes, R. N. *Pure Appl. Chem.* **1982**, *54*, 43.
(22) Wang, Z.-T.; Sinn, E.; Grimes, R. N. *Inorg. Chem.* **1985**, *24*, 826.
(23) Lipscomb, W. N. "Boron Hydrides"; Benjamin: New York, 1963.
(24) We thank Prof. Lipscomb for correspondence concerning the valence-bond structure of $B_{12}H_{16}$.
(25) Remmel, R. J.; John, H. D.; Brice, V. T.; Shore, S. G. *Inorg. Synth.* **1979**, *19*, 247.

chromatography was carried out on precoated 0.25-mm silica gel (F-254) plates.

The NMR, IR, and mass spectrometers employed in this work are described in the preceding paper.[2] Details of the NMR studies are given below.

Synthesis of Dodecaborane(16). A three-necked round-bottom flask containing 0.37 g of KH (9.3 mmol) and fitted with two tip-in tubes (similar to Figure 7 in ref 2) was evacuated. In one tube was 0.66 g of $FeCl_2$ (5.2 mmol), and in the other was 1.63 g of $FeCl_3$ (10 mmol). Hexaborane (9.2 mmol) was condensed into the flask at −196 °C followed by 30–50 mL of dimethyl ether. The flask was warmed to −78 °C and stirred for ~1 to effect deprotonation of B_6H_{10}. The contents of the flask were frozen at −196 °C, H_2 was pumped away, and the $FeCl_2$ was added in vacuo via the tip-in tube. The flask was again warmed to −78 °C and stirred at this temperature. After 1 h, $FeCl_3$ was added, and the reaction mixture was stirred a further 1–2 h. The solvent was distilled through a trap at −78 °C and into another flask at −196 °C. When the volume of solvent in the reactor had been reduced to several milliliters, the flask was allowed to come to room temperature. At this point, 0.35 g of hexaborane (4.6 mmol) had collected in the −78 °C trap, and the residue was extracted in air with 50 mL of hexane. The solvent was stripped from the extract, and the oily solid which remained was sublimed twice under vacuum to give 0.14 g (0.96 mmol) of $B_{12}H_{16}$.

Deprotonation of Dodecaborane(16). A 44-mg sample (0.30 mmol) of $B_{12}H_{16}$ and 44 mg (1 mmol) of KH were stirred at −78 °C in THF in vacuo. After 1 h, 0.17 mmol of H_2 had evolved. The reactor was allowed to warm slowly to room temperature and stirred for another 30–40 min. A slight yellowing of the solution was observed, indicating some decomposition. The total pressure of evolved H_2 was 54 torr in an apparatus volume of 85 mL, at a temperature of 295 K, corresponding to 0.25 mmol of H_2.

Regeneration of $B_{12}H_{16}$ from $B_{12}H_{15}^-$. The THF solution of $K^+B_{12}H_{15}^-$ from the preceding reaction was filtered under vacuum to remove excess KH. Excess HCl (0.9 mmol) was condensed onto the solution frozen at −196 °C. The solution was warmed to −78 °C and stirred for 1 h. The solvent was removed under vacuum, leaving yellow and white solid residues. The residue was extracted with hexane, and the hexane was removed to give a white solid which was sublimed under vacuum to give 0.027 g of crystalline material, identified by ^{11}B NMR as $B_{12}H_{16}$, corresponding to 61% yield based on the original $B_{12}H_{16}$ employed in the deprotonation. The ^{11}B NMR spectrum of an acetone rinse of the residue remaining after hexane extraction revealed mainly boric acid and small amounts of other unidentified boron species. Signals appear at δ 27.7 (d), −15.6 (d), and −16.1 (d or s). The δ −15.6 and −16.1 signals are poorly resolved.

NMR Experiments. The ^{11}B and ^1H NMR spectra were obtained by using the standard Nicolet procedure 1 PULS. Broad-band decoupling of protons from ^{11}B resonances was achieved by irradiating at the proton frequency, 360 MHz. ^{11}B NMR spectra were collected over a sweep width of ±50 000 Hz from −432 to +432 ppm. ^1H NMR spectra were routinely collected from −30 to +30 ppm.

The ^{11}B 2D NMR spectra were obtained via the COSY16 experiment.[26] Workup of the data was accomplished with the macros HOMOCSCM PROCESS 2MS 2ZF to generate the $M(\omega_1,\omega_2)$ data set and the plotting macros CONTOUR PLOT ON RASTER AND JEENER CT PLOT.[26]

The T_1 measurements were obtained with the standard Nicolet experiment T_1 IRCA, the inversion recovery technique with compensated 180° pulses and phase alternation of the 90° pulses. Workup of the raw data was accomplished with the Nicolet T_1 3IR data reduction routine, a three-parameter fit of an exponential equation.

X-ray Structure Determination on $B_{12}H_{16}$. Crystals grown by sublimation were mounted in glass capillaries and examined by precession photography, from which a crystal suitable for data collection was selected. Table II lists the relevant parameters and crystal data.

The cell dimensions and space group were obtained by standard methods on an Enraf-Nonius four-circle CAD-4 diffractometer equipped with a graphite monochromator. The θ–2θ scan technique was used, as previously described,[27] to record the intensities for all nonequivalent reflections for which $1.5° < 2\theta < 50°$. Scan widths were calculated as $(A + B \tan \theta)$, where A is estimated from the mosaicity of the crystal and B allows for the increase in peak width due to $K\alpha_1 - K\alpha_2$ splitting. The values of A and B were 0.6 and 0.35, respectively.

The intensities of three standard reflections showed no greater fluctuations during the data collection than those expected from Poisson statistics. The raw intensity data were corrected for Lorentz polarization but not for absorption, as the absorption correction was negligible. Of the 1325 independent intensities, there were 1021 with $F_o^2 > 3\sigma(F_o^2)$, where F_o^2 was estimated from counting statistics.[28] These data were used in the final refinement of the structural parameters.

The direct methods program MULTAN 74 was used to determine the nonhydrogen atom positions. Full-matrix least-squares refinement was carried out as previously described.[27] Anisotropic temperature factors were introduced for the non-hydrogen atoms. Further Fourier difference functions permitted location of all hydrogen atoms, which were included in the refinement of four cycles of least squares and then held fixed.

The model converged to the R values given in Table II. A final Fourier difference map was featureless.

Acknowledgment. This work was supported by the U.S. Army Research Office.

Supplementary Material Available: Listings of observed and calculated structure factor amplitudes, anisotropic thermal parameters, and unit cell packing diagram (7 pages). Ordering information is given on any current masthead page.

(26) This and other routines cited are available on request.

(27) Freyberg, D. P.; Mockler, G. M.; Sinn, E. *J. Chem. Soc., Dalton Trans.* **1976**, 447.

(28) Corfield, P. W. R.; Doedens, R. J.; Ibers, J. A. *Inorg. Chem.* **1967**, *6*, 197.